Conférence Internationale des Energies Renouvelables (CIER'13), Sousse, Tunisie - 2013

Vol.2
ISSN : 2356-5608

Broken Bars Effects of Induction Generator on a Wind Conversion System

R. ABDELLI[#1], D.REKIOUA[#1], A.BOUZIDA[*2]

[#]*Electrical Engineering Department, Abderrahmane MIRA (BEJAIA) University*
Address Including Country Name
[1]abdelli-radia@yahoo.fr

[*]*National Polytechnic School, Algiers*
Address Including Country Name
[2]bouzida.umbb@gmail.com

***Abstract*— This paper presents a method to study the effect of the broken bars defects of an induction generator used in a wind conversion system. The conventional three-phase model can't be applied to the induction generator's rotor in the case of defect because it can't determine the instantaneous properties of rotor bars. Thus for introducing the broken information, we apply the Magnetically Coupled Circuits Approach (MCCA) which allows us to show the broken bars effects on the wind conversion performances in order to predict diagnosis methods to protect this system.**

***Keywords*— Induction generator, Broken bars, Rotor defects, Magnetically Coupled Multiple Circuits Approach.**

I. INTRODUCTION

Actual strategies for sustainable energy development have a prior objective the gradual replacement of fossil-fuel-based energy sources by renewable energy ones. Among the clean energy sources, wind energy conversion systems currently carry significant weight in many developed countries [1-2].

The majority of wind turbines installed in grid connected applications use induction generators [6]. An induction generator operates within a narrow range of speeds slightly higher than its synchronous speed. The main advantage of induction generator is that they are rugged, inexpensive, and easy to connect to an electrical network.

The rotor defects are often due to the electromagnetic torque and rotation speed ripples. The broken bars constitute a considerable part of the induction machine defects. This problem generally does not cause the final stopping of the machine but it can generate serious side effects [7-8]. In the case of a wind conversion system based on an induction generator, this problem must be taken into account since the power sent to the network will be affected, The broken bars information is transported by the magnetic flux to the stator, and consequently by the current sent to the network [9-11].

For electrical machines and especially induction motors, the broken bars faults and their diagnosis techniques are reported in a great number of papers [7-11], in this work, the effect of an induction generator broken bars defect on the wind conversion system performances is presented. Since the setting in equation of these defects cannot be done by the classical model in the Park reference, the Multiple Coupled Circuit Approach is used in order to introduce the rotor defect into the machine model. The obtained simulation results showing the effect of the broken bars of an induction generator in a wind system connected to the electrical network through PWM static inverters [12-13] are presented and discussed.

II. WIND CONVERSION SYSTEM MODEL

The studied system is presented in (Fig.1)

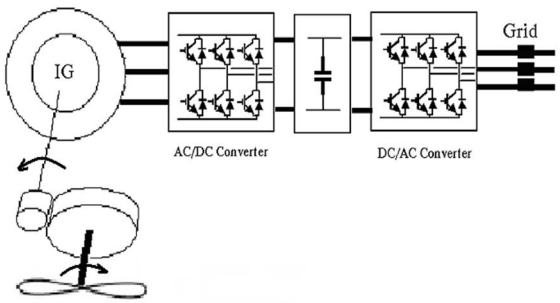

Fig.1. Wind generator based on a cage induction generator

A. Wind Turbine Model

Considering a wind average velocity v and a multiplier gain G, supposed without losses, the mechanical torque of the generator can be expressed, in a classical way, as follows:

$$T_g = \frac{1}{2} C_p(\lambda) \rho S \frac{v^3}{G\omega_t} \qquad (1)$$

Where S is the turbine section ($S = \pi R^2$), ρ represents the air density, $C_p(\lambda)$ is the performance coefficient, λ is defined as:

$$\lambda = \frac{\omega_t . R}{v} \qquad (2)$$

Where λ is the tip-speed ratio, ω_t (rad/s) is the turbine angular speed and R is the blade radius.

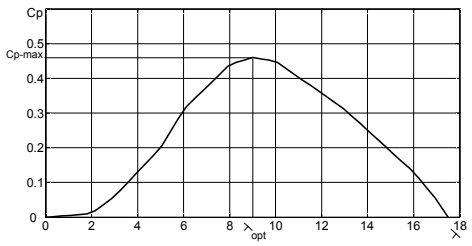

Fig.2. Characteristic $C_P(\lambda)$

The characteristic $C_P(\lambda)$, given by the turbine manufacturer, is of a parabolic form for the pitch angle β=0 with a maximal value $C_{P\text{-max}}$ for λ_{opt}. The generator speed is then controlled thanks to an algorithm allowing the maximum extraction of the power (MPPT: Maximum Power Point Tracking [33-34]). This one requires the measure or estimation of the wind speed knowing that to a given wind speed v corresponds an optimal tip-speed ratio λ_{opt} and then a maximal power. In this case, the electromagnetic torque reference T_{e-ref} can be expressed as:

$$T_{e-ref} = \frac{C_{P-\max}}{\lambda_{opt}^3}\frac{\rho}{2}\pi\frac{R^5}{G^3}.\omega_m^2 \tag{3}$$

Where ω_m is the mechanic generator speed.

B. Speed Multiplier Model

The speed multiplier is used to adapt the turbine rotation speed ω_t to the generator one. It is described by the two following equations:

$$T_t = \frac{T_g}{G} \quad and\, \omega_t = \frac{\omega_m}{G} \tag{5}$$

Where: T_t and T_g are respectively the turbine and generator torques.

C. Transmission Elements Model

The basic principle of dynamics gives:

$$T_{e-ref} - T_g = J\frac{d\omega_m}{dt} + f\omega_m \tag{6}$$

Where f and J are the friction coefficient and the system moment of inertia respectively.

D. Induction Generator Model

The modelling of the induction squirrel-cage machine using the three-phase model cannot determine the instantaneous real currents circulating in the rotor bars. This model can't introduce the defects in the rotor model. In the literature, different models have been introduced to take into account the defects in the rotor [18-20]. In this paper the magnetically coupled circuits approach is developed [21-22]. In this method, the rotor model is composed of as many phases as bars so the currents circulating in the rotor meshes are considered as phase currents of the rotor.

1) Stator Equations:

The stator electric equation is:

$$[V_s] = [R_s][I_s] + \frac{d[\Phi_s]}{dt} \tag{8}$$

With: $[V_s] = [v_a \quad v_b \quad v_c]^T$, $[I_s] = [i_a \quad i_b \quad i_c]^T$,

The resistances matrix $[R_s]$ contains each winding resistance:

$$[R_s] = \begin{bmatrix} R_s & 0 & 0 \\ 0 & R_s & 0 \\ 0 & 0 & R_s \end{bmatrix}$$

The total stator flow matrix $[\Phi_s]$ is represented by:

$$[\Phi_s] = [\Phi_{ss}] + [\Phi_{sr}] \tag{9}$$

Φ_{ss} and Φ_{sr} are the stator flow due to the stator currents and the rotor currents respectively.

For a winding sinusoidal distribution, the matrix $[\Phi_{ss}]$ is expressed by:

$$[\Phi_{ss}] = \begin{bmatrix} \Phi_{ass} \\ \Phi_{bss} \\ \Phi_{css} \end{bmatrix} = \begin{bmatrix} L_{ls}+L_{ms} & -L_{ms}/2 & -L_{ms}/2 \\ -L_{ms}/2 & L_{ls}+L_{ms} & -L_{ms}/2 \\ -L_{ms}/2 & -L_{ms}/2 & L_{ls}+L_{ms} \end{bmatrix} \begin{bmatrix} i_a \\ i_b \\ i_c \end{bmatrix} \tag{10}$$

L_{ls}, L_{ms} : are respectively the leakage and magnetising inductance of stator windings such as:

$$L_{ms} = \frac{\mu_0 . l . r}{g}.N_s^2.\frac{\pi}{4} \tag{11}$$

The stator flow due to the rotor currents is given by:

$$[\Phi_{sr}] = \begin{bmatrix} \Phi_{asr} \\ \Phi_{bsr} \\ \Phi_{csr} \end{bmatrix} = \begin{bmatrix} L_{a1} & L_{a2} & \dots & \dots & L_{aNr} \\ L_{b1} & L_{b2} & \dots & \dots & L_{bNr} \\ L_{c1} & L_{c2} & \dots & \dots & L_{cNr} \end{bmatrix} \begin{bmatrix} i_{r1} \\ i_{r2} \\ . \\ . \\ i_{rNr} \end{bmatrix} \tag{12}$$

The stator-rotor mutual inductances matrix is:

$$[L_{sr}] = L_m \begin{bmatrix} \cos(\theta_r+\delta) & \cos(\theta_r+\alpha_r+\delta) & .. & \cos(\theta_r+(N_r-1)\alpha_r+\delta) \\ \cos\left(\theta_r+\delta-\frac{2\pi}{3}\right) & \cos\left(\theta_r+\alpha_r+\delta-\frac{2\pi}{3}\right) & .. & \cos\left(\theta_r+(N_r-1)\alpha_r+\delta-\frac{2\pi}{3}\right) \\ \cos\left(\theta_r+\delta+\frac{2\pi}{3}\right) & \cos\left(\theta_r+\alpha_r+\delta+\frac{2\pi}{3}\right) & .. & \cos\left(\theta_r+(N_r-1)\alpha_r+\delta+\frac{2\pi}{3}\right) \end{bmatrix}$$

With: $L_m = \frac{4.L_{ms}}{\pi.N_s}\sin\delta$, $\alpha_r = \frac{2.\pi}{N_r}$, $\delta = \frac{N_r}{2}$

2) Rotor Equations

The rotor cage of an induction machine is represented by an equivalent circuit having (N_r) meshes. Each mesh is defined by two adjacent rotor bars connected between them by an end-ring. Each bar and each end-ring are replaced by an equivalent circuit represented by a resistance and an inductance. From these equivalent circuits, we can give the following rotor electric equation:

$$\begin{bmatrix}0\\0\\.\\.\\0\end{bmatrix}=\begin{bmatrix}R_0 & -R_b & 0 & . & -R_b\\ -R_b & R_0 & . & . & 0\\ 0 & . & . & . & .\\ . & . & . & . & .\\ -R_b & . & . & -R_b & R_0\end{bmatrix}\begin{bmatrix}i_{r1}\\i_{r2}\\.\\.\\i_{rNr}\end{bmatrix}+\frac{d}{dt}\begin{bmatrix}\phi_{r1}\\\phi_{r2}\\.\\.\\\phi_{rNr}\end{bmatrix} \quad (14)$$

The total rotor flow matrix is given by:

$$[\Phi_r]=[\Phi_{rr}]+[\Phi_{rs}] \quad (15)$$

Φ_{rr} and Φ_{rs} are rotor flow due to the rotor currents and the stator currents respectively.

Φ_{rs} is given by the following equation :

$$[\Phi_{rs}]=[L_{sr}]^T.\begin{bmatrix}i_a\\i_b\\i_c\end{bmatrix} \quad (16)$$

$$[\Phi_{rr}]=\begin{bmatrix}L_0 & L_{12}-L_b & L_{13} & . & L_{1(Nr-1)} & L_{1Nr}-L_b\\ L_{21}-L_b & L_0 & L_{23}-L_b & . & . & L_{2Nr}\\ L_{31} & L_{32}-L_b & . & . & . & .\\ . & . & . & . & . & .\\ . & . & . & . & . & L_{(Nr-1)Nr}-L_b\\ L_{Nr1}-L_b & . & . & . & L_{Nr(Nr-1)}-L_b & L_0\end{bmatrix}\begin{bmatrix}i_{r1}\\i_{r2}\\.\\.\\.\\i_{rNr}\end{bmatrix} \quad (17)$$

With:

$$R_0=2.(R_b+R_e)\ ,\quad L_0=L_{kk}+2.(L_b+L_e) \quad (19)$$

$$L_{kk}=\frac{\mu_0.l.r}{g}.\alpha_r.\left(1-\frac{\alpha_r}{2.\pi}\right)\quad L_{ki}=\frac{\mu_0.l.r}{g}.\left(\frac{-\alpha_r^2}{2.\pi}\right) \quad (21)$$

R_b and R_e are respectively bar and end-ring circuit resistance.

The bars currents are expressed according to the rotor currents by the following relation deduced by the application of Kirchhoff's laws:

$$i_{bk}=i_{rk}-i_{r(k+1)} \quad (23)$$

Electromagnetic torque T_{em} expression is given by the magnetic co-energy:

$$T_{em}=\frac{p}{2}[I_s]^T\frac{\partial[L_{sr}]}{\partial\theta_r}[I_r] \quad (24)$$

3) Introduction of the rotor defects to the induction generator model

The broken bar in the rotor imposes a change in equations and especially in the calculation of self and mutual inductances and resistance [23-24].

In the generalized model for k adjacent broken bars in the rotor, the number of rotor equations is decreased according to the number of broken bars and the meshes concerned by the rupture are eliminated, the mesh j will be (k+1) times boarder.

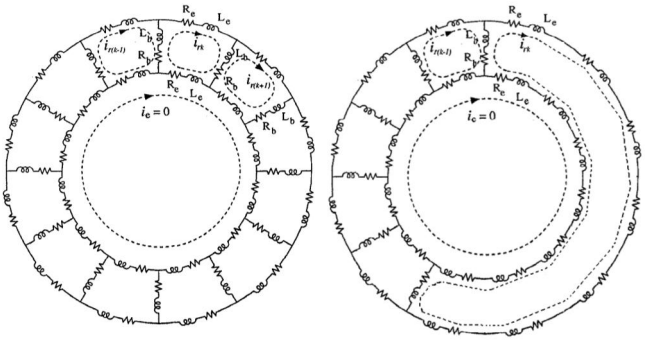

Fig.4. Equivalent rotor circuit of the induction generator, a healthy rotor (left) and rotor with k adjacent broken bars (right)

The self inductance corresponding to the mesh j is:

$$L_{0j}=\frac{\mu_0.l.r}{g}.\alpha_r.\left((k+1)\frac{(2k+1).\alpha_r}{2.\pi}\right)+2\left(L_b+(k+1)L_e\right) \quad (32)$$

The mutual rotor- rotor inductance L_{rirj} is in this case:

$$L_{rirj}=-(k+1).\frac{\mu_0.l.r}{g}.\frac{\alpha_r^2}{2.\pi} \quad (33)$$

The mutual inductance L_{aj} between the stator winding (a) and the mesh j is obtained from:

$$L_{aj}=L_m.\cos(\theta_r+(k+1).(j-1).\alpha_r+\delta) \quad (34)$$

The rotor resistances matrix is also affected by the breakdown; it is obtained from this new representation:

$$[R_r]'=\begin{bmatrix}R_0 & -R_b & . & . & 0 & 0 & . & . & 0 & -R_b\\ -R_b & R_0 & . & . & . & . & . & . & . & 0\\ . & . & . & . & . & . & . & . & . & .\\ . & . & . & . & -R_b & . & . & . & . & .\\ . & . & . & -R_b & 2.(R_b+(k+1).R_e) & -R_b & . & . & . & .\\ . & . & . & . & -R_b & R_0 & -R_b & . & . & .\\ . & . & . & . & . & -R_b & . & . & . & .\\ . & . & . & . & . & . & . & . & . & .\\ -R_b & 0 & . & . & 0 & 0 & . & . & -R_b & R_0\end{bmatrix} \quad (35)$$

$$R_{0j}=2.(R_b+(k+1).R_e) \quad (36)$$

E. AC/DC Converter Model

The AC/DC rectifier model is expressed by the two following equations:

$$\begin{pmatrix}V_a\\V_b\\V_c\end{pmatrix}=\frac{V_{dc}}{3}\begin{pmatrix}-2 & 1 & 1\\ 1 & -2 & 1\\ 1 & 1 & -2\end{pmatrix}\begin{pmatrix}S_a\\S_b\\S_c\end{pmatrix} \quad (37)$$

$$i_{dc}=S_a i_a+S_b i_b+S_c i_c \quad (38)$$

With: V_{dc} and i_{dc} are the direct bus voltage and current respectively. (S_a,S_b,S_c) are the logic functions according to

the switch states obtained by the application of the PWM control (Fig.???).

F. Direct Bus Voltage Model

The instantaneous change in direct bus voltage V_{dc} is given by the capacitive current i_c integration.

$$V_{dc} = \int \frac{1}{C} i_c dt \tag{39}$$

with: $i_c = i_{dc} - i_n$ (40)

And $i_n = F_1 i_{n1} + F_2 i_{n2} + F_3 i_{n3}$ (41)

F_1, F_2, F_3 are logic functions according to the switch states given by the grid link control (Fig.5) and i_{n1}, i_{n2}, i_{n3} are the three phase currents supplied to the grid.

G. DC/AC Converter and Grid Link Model and Control

The inverter is modeled in the same manner as the previous rectifier:

$$\begin{pmatrix} V_{in1} \\ V_{in2} \\ V_{in3} \end{pmatrix} = \frac{V_{dc}}{3} \begin{pmatrix} -2 & 1 & 1 \\ 1 & -2 & 1 \\ 1 & 1 & -2 \end{pmatrix} \begin{pmatrix} F_1 \\ F_2 \\ F_3 \end{pmatrix} \tag{42}$$

$V_{in1}, V_{in2}, V_{in3}$ being the three phase voltages of the DC/AC inverter. Then the filter, constituted of R_n and L_n, links these voltages to E_1, E_2, E_3, which are the three phase voltages of the grid, through the following relation:

$$\begin{pmatrix} V_{in1} \\ V_{in2} \\ V_{in3} \end{pmatrix} = R_n \begin{pmatrix} i_{n1} \\ i_{n2} \\ i_{n3} \end{pmatrix} + L_n \frac{d}{dt} \begin{pmatrix} i_{n1} \\ i_{n2} \\ i_{n3} \end{pmatrix} + \begin{pmatrix} E_1 \\ E_2 \\ E_3 \end{pmatrix} \tag{43}$$

The control scheme of the inverter is presented in Fig.5. The grid link control consists in adjusting the active power supplied to the grid to its reference value P_{ref} and the reactive power Q_{ref} to zero in order to fix the power factor at the unit. The active power reference is deduced by controlling the direct bus voltage with a proportional integral corrector generating the current reference i_{c-ref} to the capacity (Fig.5).

Hence, we can express P_{ref} as:

$$P_{ref} = V_{dc}.(i_{dc} - i_{cref}) \tag{44}$$

Thus: $P_{ref} = P_{dc} - P_{cref}$ (45)

With: $i_{cref} = PI.(V_{dc-ref} - V_{dc})$ (46)

The reference active and reactive powers are given by the following equations:

$$P_{ref} = E_d i_{nd\_ref} + E_q i_{nq\_ref}, Q_{ref} = E_q i_{nd\_ref} - E_d i_{nq\_ref} \tag{48}$$

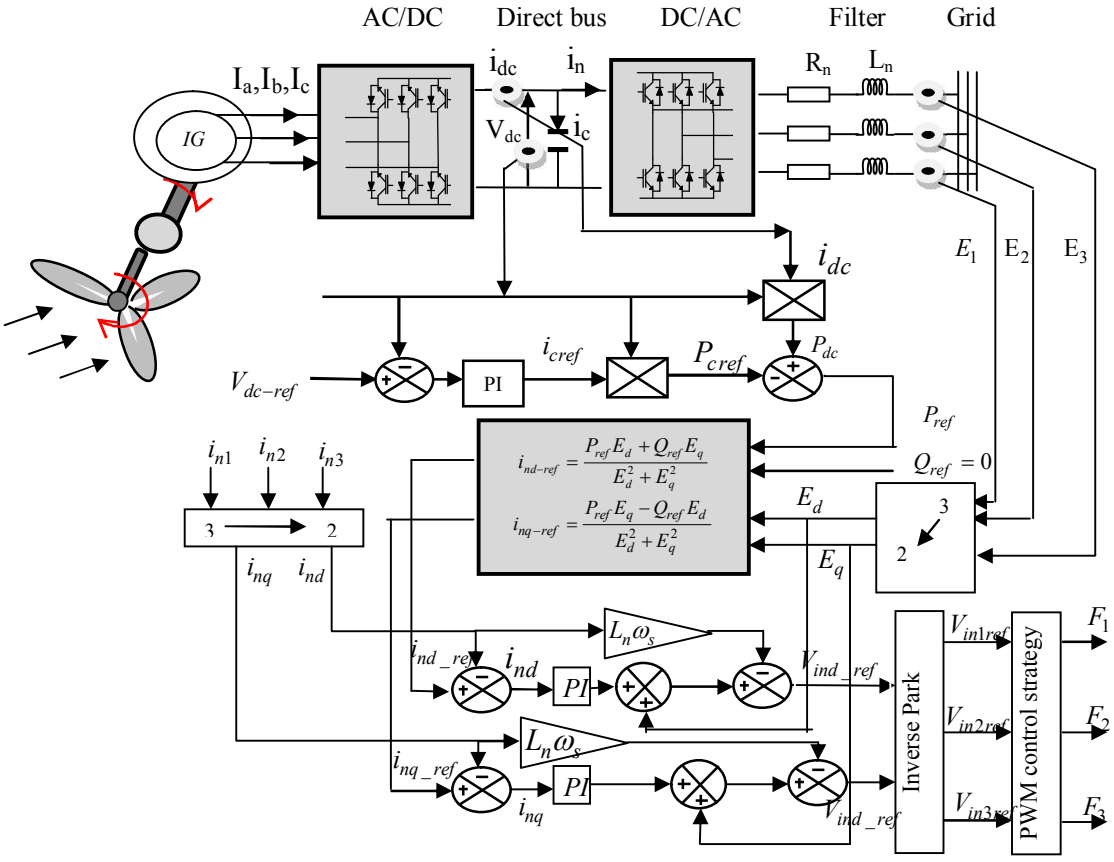

Fig.5. Direct bus and power control

Then, multiplying Eq.47 by E_d and Eq.48 by E_d, the addition and subtraction of the two resulting equations give the reference current value according to active and reactive power ones by:

$$i_{nd-ref} = \frac{P_{ref}E_d + Q_{ref}E_q}{E_d^2 + E_q^2} \quad , i_{nq-ref} = \frac{P_{ref}E_q - Q_{ref}E_d}{V_d^2 + V_q^2} \tag{49}$$

Where: E_d, E_q are the Park components of E_1, E_2, E_3.

III. Simulation Results

The simulation of the studied system is made under Matlab/Simulink environment. We compare the continuous bus voltage (Fig.7), electromagnetic torque (Fig.8), active power sent to the network (Fig.9) and currents (Fig.10 and 11) in the case of a healthy generator, then in the case of a two broken bars and 8 broken bars generator.

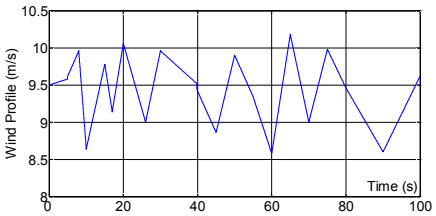

Fig.6 Wind Speed

The continuous bus voltage is regulated in order to maintain its value constant by the application of the proportional integral corrector, but its allure move away from its reference value with the break of bars (80% in case of two broken bars), this problem is as large as the number of broken bars (until 400% in the case of height broken bars)(Fig.7).

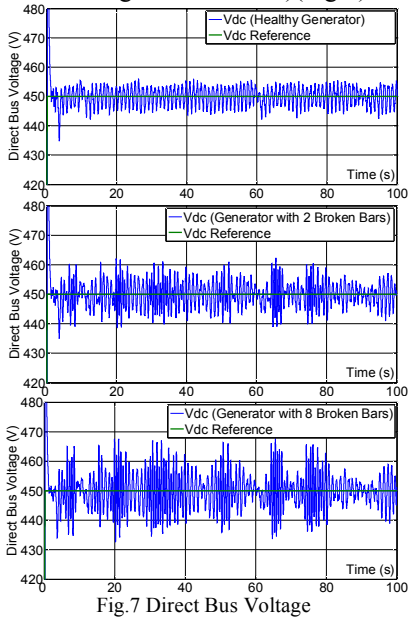

Fig.7 Direct Bus Voltage

Fig.8 shows that the electromagnetic torque ripples are increasingly strong with number of broken bars (200% in the case of two broken bars and until 500% in the case of height broken bars); these mechanical undesirable effects translate considerable vibrations which generate acoustic harmful effects and can lead to new rotor failures. These problems are led to the stator by the magnetic flow and consequently to the electrical grid (Fig.9,10,11).

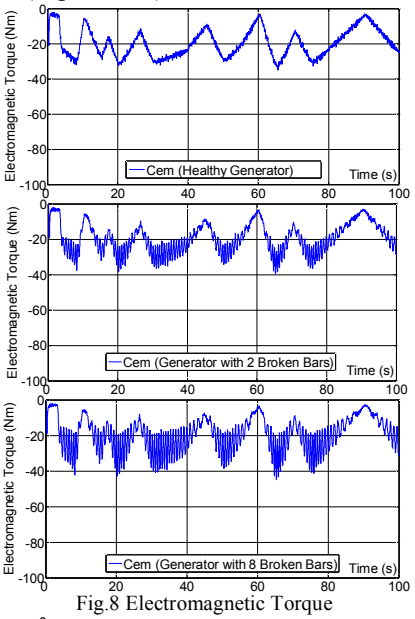

Fig.8 Electromagnetic Torque

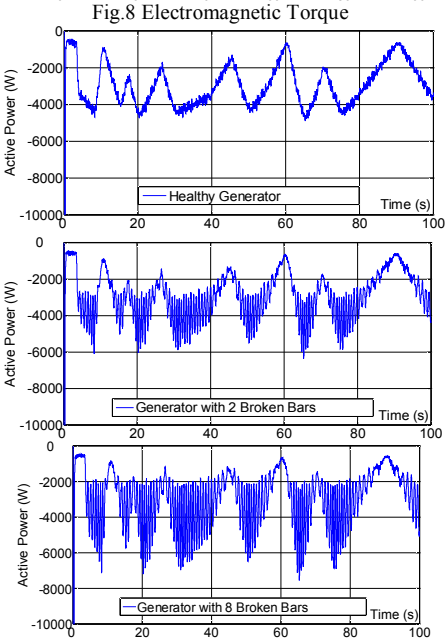

Fig.9 Active Power sent to the Grid

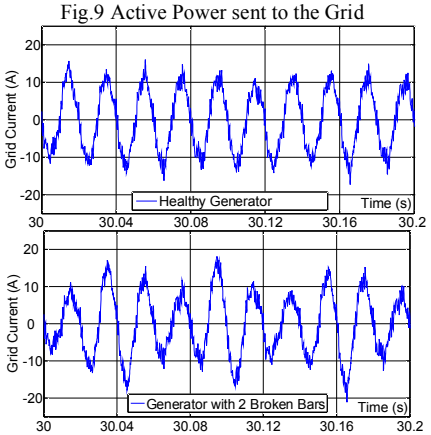

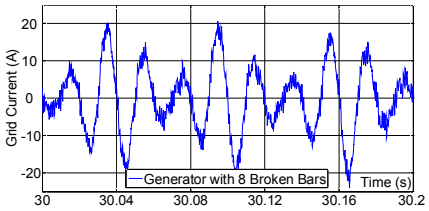

Fig.10 Current Sent to the Grid

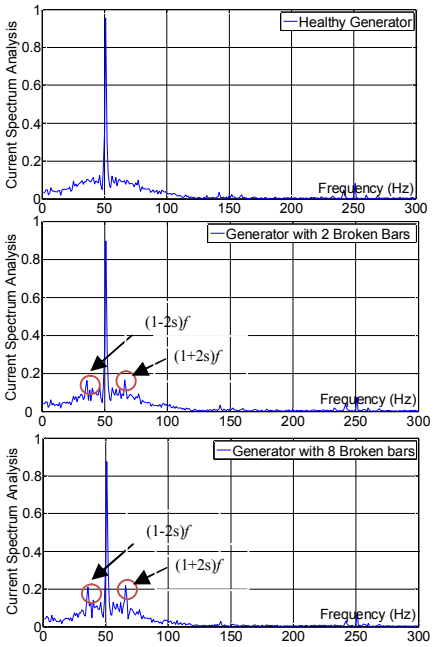

Fig.11 Spectrum Analysis of the Current Sent to the Grid

The current spectral analysis (Fig.11) shows an appearance of symmetrical harmonics around the fundamental frequency (f=50 Hz). The magnitude of these harmonics is as important as the number of broken bars is important (0.06 in the case of two broken bars and 0.12 in the case of height broken bars). This analysis is presented in many works [8-11] as diagnosis method to identify rotor bar faults.

IV. Conclusion

In this present paper, we have presented the broken bars effects of an induction generator in the case of a wind conversion system. We note that in the case of bars ruptures, all controlled parameters (continuous bus voltage, electromagnetic torque, active power) move away from their references and present a considerable unbalances in their waveforms. This problem is directly proportional to the number of broken bars.

Appendix

Wind turbine parameters

Rated power	7.5 KW	Rated speed	296 rd/mn
Radius	3.24m	Multiplier gain	3.1475

Generator parameters

Rated power	4 KW	Number of rotor bars	28
Rated voltage	220/380 V	End-ring inductance	0.0033µH
Rated speed	1435rd/mn	End-ring resistance	1.21 µΩ
Stator leakage inductance	0.0042H	Number of pole pairs	2
Bar inductance	0.67µH	Rotor bar resistance	79.4 µΩ

References

[1] A. Ouammi, H. Dagdaoui, R. Sacile, A. Mimet. « Monthly and seasonal assessment of wind energy characteristics at four monitored locations in Liguria region (Italy) ». Renewable Energy Reviews, Vol 14, Issue 7, pp 1959-1968, Sep 2010.

[2] O.V. Marchenko, S.V. Solomin. « Efficiency of wind energy utilization for electricity and heat supply in northern regions of Russia ». Renewable Energy, vol 29, Issue 11, pp 1793-1809, Sep 2004.

[6] M.N. Mansouri, M.F. Mimouni, B. Benghanem, M. Annabi. « Simulation model for wind turbine with asynchronous generator interconnected to the electric network », *Renewable Energy, Vol 29, Issue 3, pp 421-431, Mar 2004.*

[7] M. E. H. Benbouzid. « Bibliography on Induction Motors Faults Detection and Diagnosis», *IEEE Transactions on Energy Conversion, Vol 14 n°4, pp 1065-1074, Dec 1999.*

[8] A. H. Bonnett, G. C. Soukup. « Cause and Analysis of Stator and Rotor Failures in Three Phase Squirrel Cage Induction Motors », *IEEE Transactions on Industry Applications, Vol 28, n°4 Jul/Aug 1992.*

[9] M. E. H. Benbouzid, M. Vieira, C. Theys. « Induction motors faults detection and localization using stator current advanced signal processing techniques », *IEEE Transactions on Power Electronics, Vol 14, n°1 pp 14-22 Jan 1999.*

[10] O. Touhami, L. Noureddine, R. Ibtiouen. « Spectral analysis for the rotor defects diagnosis of an induction machine », *IEEE-WISP, Portugal pp 183-187,Sep 2005.*

[11] J. F. Bangura, N. A. Demdash. «Diagnosis and characterization of effects of broken bars and connectors in squirrel-cage induction motors by a time-stepping coupled finite element-state space modeling approach », *IEEE Transactions on Energy Conversion, Vol 14, n°4 pp 1167-1176 Dec 1999.*

[12] F. D Bianchi, H. De Battista, R. J. Mantz. « Wind turbine control system », *London, Springer-Verlag, 2007.*

[13] S. El Aimani. « Modélisation de différentes technologies d'éoliennes intégrées dans un réseau de moyenne tension », *Thèse de Doctorat de l'école centrale de Lille, France, 2004.*

[18] X. Luo, Y. Liao, H. A. Toliyat, A. El-Antably, T. A. Lipo. « Multiple Coupled Circuit Modeling of Induction Machines », *IEEE Transactions on Industry Applications, Vol 31 n°2, pp 311-318, Mar/Apr 1995.*

[19] H. Henao, C. Martis, G-A. Capolino. « An equivalent internal circuit of the induction machine for advanced spectral analysis », *IEEE Transactions on Industry applications, Vol 40 n°3, pp 726-734, 2004.*

[20] J.F. Bangura, N.A. Demerdash. « diagnosis and characterization of effects of broken bars and connectors in squirrel cage induction motors by a time-stepping coupled finite element-state space modeling approach », *IEEE Transactions on Energy conversion, vol 14 n°4, pp 1167-1176, 2002.*

[21] O. Touhami, L. Noureddine, R. Ibtiouen, M. Fadel. « Modeling of the Induction Machine for the Diagnosis of Rotor Defects », *IEEE, Industrial Electronics Society, Part I (pp 1580-1587), part II (pp 1621-1626), IECEN 2005.*

[22] G. Houdouin, G.Barakat, B. Dakyo, E. Destobbeleer. « A Winding Function Theory Based Global Method for the Simulation of Faulty Induction Machines », *IEEE, Electrical Machines and Drives, pp 297-303, 2003.*

[23] G. Didier. « Modélisation et Diagnostic de la Machine Asynchrone en présence de Défaillances », *Thèse de Doctorat en Génie Electrique, Université Henri Poincaré, Nancy I. Oct 2004.*

[24]H. A. Toliyat, T. A. Lipo. « Transient Analysis of cage Induction Machines under Stator, Rotor, Bar and End-Ring Faults », *IEEE Transactions on Energy Conversion, Vol 10 n°2, pp 241-247.1995.*